Systematic calorimetric investigation of the effect of silica aerosils on the nematic to isotropic transition in heptylcyanobiphenyl

P. Jamée, G. Pitsi, and J. Thoen
Laboratorium voor Akoestiek en Thermische Fysica, Departement Natuurkunde en Sterrenkunde, Katholieke Universiteit Leuven, Celestijnenlaan 200D, B-3001 Leuven, Belgium
(Received 12 March 2002; published 16 August 2002)

The effect of confinement on liquid crystal phase transitions was investigated in mixtures of the liquid crystal heptylcyanobiphenyl with hydrophilic aerosils. The influence of the aerosil density on the nematic to isotropic transition was studied by adiabatic scanning calorimetry. Mixtures have been investigated with an aerosil content between $\rho_S = 0.1$ and $\rho_S = 0.7$, the latter being substantially higher than that investigated in previous studies with other liquid crystal-aerosil mixtures. The transitions in the examined mixtures exhibited an unusually large broadening, while the transition temperatures showed peculiar behavior. Notwithstanding, the transition (latent) heat behaved as could be expected on the basis of previous studies. The observed behavior can be explained, in the context of the elastic-strain approach usually employed to describe transition temperature shifts, by variations in the distribution of the radius of curvature R of the aerosil voids originating from sample preparation. It is important in this regard to separate the behavior of the transition temperatures and the transition (latent) heats, the former being influenced by the radius of curvature of the voids and the latter by the total void surface per unit volume. Three quantitative models were compared with experimental results. Both the pinned boundary layer and the random field model yield an evolution of transition temperatures not in agreement with experimental observations. More importantly, they predict a decrease of the pretransitional specific heat capacity, not supported by experiment. The difficulties with these models are avoided in a third, mean-field surface-induced order model.

DOI: 10.1103/PhysRevE.66.021707 PACS number(s): 61.30.Pq, 64.70.Md

I. INTRODUCTION

The transition between the nematic and isotropic phase in liquid crystals has been extensively studied in the past [1–3]. A recent topic of interest is the influence on this and other phase transitions of the addition of aerosil particles. Aerosils are very small (typically 10 nm) silica particles, whose surface has been treated so that they obtain a hydrophilic or hydrophobic character. Hydrophilic aerosils form networks that, when added to a liquid crystal, disturb its ordering in a random manner. By varying the added amount of aerosils, one can thus study in a controlled manner the influence of an increasing random disturbance of the liquid crystal order. This research is part of a significant interest, both from a fundamental and a technical point of view (for example applications such as polymer dispersed liquid crystal displays), in the effects of confinement upon liquid crystal phase transitions, such as in polymer and porous materials [4] or in aerogels [5–8]. The advantage of the use of aerosils over aerogels is their greater ease of preparation and a greater variability of concentrations, together with the fragility of low-density aerogels. Several calorimetric investigations of different liquid crystal-aerosil systems have been conducted [9–14], besides structural studies using x-ray and optical methods [12,15,16].

We have made a systematic study by adiabatic scanning calorimetry of the influence of such hydrophilic aerosils on the nematic to isotropic (NI) transition in the liquid crystal heptylcyanobiphenyl (7CB), extending to higher aerosil concentrations (i.e., $\rho_S > 0.4$) than those mentioned in the existing literature concerning mixtures with other liquid crystals [9–14]. Adiabatic scanning calorimetry (ASC) is a high resolution calorimetric technique that can not only measure the specific heat capacity $C_p(T)$ of a sample, but also has the unique capability of being able to perform a direct determination of the enthalpy $H(T)$.

A systematic dielectrical study of mixtures of this type has already provided additional information about the evolution of the change in order parameter at different aerosil concentrations, as well an insight in to dynamical processes in the vicinity of the NI transition (in the frequency range of 75 kHz–30 MHz) [17]. The results of other dielectrical studies are available [18–21], but not all of them involve a systematic investigation over different aerosil concentrations.

II. ADIABATIC SCANNING CALORIMETRY

Measurements have been performed with an adiabatic scanning calorimeter consisting of three stages. The inner stage, the sample enclosed in a holder, is surrounded by the second stage which is a temperature controlled shield. This is enclosed in a third shield submerged in a water thermostat providing a good initial temperature stabilization. Fluctuations on the preset temperature difference of 5 K between the thermostat and the second stage can be limited to 15 mK, while temperature differences between inner and second stage can be controlled within ± 0.3 mK during an entire scan. Heating and cooling runs can be carried out at very slow scanning rates, typically 2 mK/min, ensuring thermodynamic equilibrium. When a known constant heating (cooling) power P is applied to the inner stage, the experimental

curve of its temperature versus time, $T(t)$, provides a direct measurement of the enthalpy change

$$H(T)-H(T_s)=\int_{T_s}^{T_{tr}} C dT+\Delta H_L+\int_{T_{tr}}^{T} C dT \tag{1}$$

$$=P(t_i-t_s)+P(t_f-t_i)+P(t-t_f), \tag{2}$$

where the subscript s refers to the starting conditions. This is a unique feature of ASC calorimetry. Upon the occurrence of a first-order transition, the sample temperature will remain essentially constant at the transition temperature T_{tr} during a finite time interval $t_f-t_i=\Delta H_L/P$, where ΔH_L is the latent heat. We clearly distinguish between the actual latent heat ΔH_L (i.e., the enthalpy jump at a first-order transition) and pretransitional enthalpy increases, whereas the total transition heat is the sum of both. It must also be noted that in practice, first-order transitions usually have a two phase coexistence region, due to impurities or inhomogenitities in the sample. This results in a broadening of the latent heat jump over a (small) temperature interval. The heat capacity C of the inner stage is the sum of that of the holder, C_h, and that of the the sample, C_s,

$$C=C_s+C_h=\frac{P}{\dot{T}}, \tag{3}$$

where $\dot{T}=dT/dt$ is obtained by numerical differentiation of $T(t)$. The specific heat capacity of the sample is thus found upon subtraction of the holder contribution and division by the sample mass. The calorimeter can also be operated in a pulse mode, which is used to check specific heat capacity background values away from a transition.

This technique has already been employed for the study of a wide variety of phase transitions in liquid crystals [3,22–24] and other systems [25,26]. Further details concerning the ASC technique can be found elsewhere [27].

III. INVESTIGATED SAMPLES

For our investigation 7 nm hydrophilic aerosil particles obtained from Degussa Corp. (Degussa-type 300 Aerosil) were used [28]. Mixtures were prepared according to a solvent procedure as described in Ref. [10], which allows for a preparation of higher-density mixtures with better reliability concerning homogeneity than the mechanical mixing procedure employed for initial aerosil work. First, aerosils are dried overnight at 200 °C under vacuum. Both aerosils and 7CB are then dissolved in acetone. In order to achieve a homogeneous dispersion of silica particles, this solution is then put in an ultrasonic bath for 1–2 h. Finally the acetone is evaporated at a temperature well above the NI transition temperature (the liquid crystal thus remaining in the isotropic phase) leaving a 7CB+sil mixture which is then added to the measurement cell. Mixtures are characterized by the aerosil density $\rho_s=m_s/V_{LC}$ (with m_s the mass of aerosils and V_{LC} the volume of the liquid crystal), which can be obtained from the mass m_{LC} and the density ρ_{LC} of liquid crystal and the aerosil mass m_s used in the sample preparation ($\rho_{LC}\cong 1\ \mathrm{g\,cm^{-3}}$ for 7CB),

$$\rho_s=\frac{m_s}{V_{LC}}=\frac{m_s}{m_{LC}}\rho_{LC}\cong\frac{m_s}{m_{LC}}\ (\mathrm{g\,cm^{-3}}). \tag{4}$$

TABLE I. Details of the investigated 7CB+aerosil samples (in order of preparation).

ρ_S (g cm^{-3})	m_{sample} (g)	m_{LC} (g)	m_s (g)
0.15	2.567	2.230	0.337
0.42	2.238	1.578	0.660
0.57	2.042	1.304	0.738
0.66	2.356	1.419	0.937
0.27	2.509	1.981	0.529
0.096	1.521	1.388	0.133
0.58	1.920	1.215	0.705

Mixtures were prepared with (in chronological order) $\rho_S=0.15$, 0.42, 0.57, 0.66, 0.27, 0.096, and 0.58 g cm^{-3}. For reasons of comparison, one pure 7CB sample was also investigated. Further details can be found in Table I.

Due to the hydrophilic nature of the aerosils, caution must also be taken to minimize the possibility of absorbing water into the sample. In the 0.15, 0.42, and 0.57 samples, aerosils were briefly (≈ 5 min) exposed to air during weighing as well as the dissolved mixture during the first evaporation step. This was further optimized by performing the complete sample preparation of the following mixtures under nitrogen atmosphere. A secondary source for (possible) sample impurities are contaminations in the acetone used (purity 99.8%).

One must note that, due to the nature of our ASC setup, quite large sample quantities of around 2 g are used. During the course of these measurements, steps were taken in order to optimize the above described mixing procedure to this situation. First, the evaporation procedure was split in two steps, the first being a slow evaporation (typically around 12 h). The second step then consists of placing the sample under 10^{-2} Torr vacuum for about 12 h in order to eliminate any leftover acetone from the sample.

During the course of the experiments some doubt arose about the homogeneity of the produced samples, because of the large amounts prepared and the often high aerosil densities. As a precautionary measure, in the 0.27, 0.096, and 0.58 mixtures the first evaporation step was shortened to ≈ 4 h. During this preparation step the mixture was magnetically stirred.

IV. THEORETICAL MODELS

A first theoretical model for the NI transition in liquid crystal-aerosil mixtures is a pinned-boundary-layer (PBL) model [12]. One assumes that a fraction p of the mixture, which is fully quenched, is very strongly anchored at the boundary with the aerosil strands, thus this fraction does not

undergo any phase transition while the rest of the mixture behaves as bulk liquid crystal. Consequently, the latent heat of such a mixture is described by $\Delta H_L(p)=\Delta H_L(0)(1-p)$ while the transition temperature T_{NI} remains unaltered. Naturally, the pretransition δH also reduces as $\delta H(p)=\delta H(0)(1-p)$.

Second, the random-field (RF) model again supposes a quenched fraction p, but now randomly distributed over the sample. In a mean-field approach, the NI latent heat is equal to $\Delta H_L=(a_0/2)Q_N^2 T_{NI}$, Q_N being the order parameter of the nematic phase at T_{NI} (where the order parameter Q_I of the coexisting isotropic phase is taken as zero) and a_0 the leading-order Landau–de Gennes free-energy expansion coefficient. The volume-averaged order $\overline{Q}(p)$ of the nematic phase is found to be $\overline{Q}(p)=Q(0)(1-p)$, where $Q(0)$ is the bulk order parameter at T_{NI} [29,30]. The temperature shift of the NI transition is described by $T_{NI}(p)=T_{NI}(0)(1-p)$ [29,30]. Thus one obtains $\Delta H_L(p)=\Delta H_L(0)(1-p)^3$ for the latent heat while $\delta H(p)=\delta H(0)(1-p)$ for the same reason as in the PBL model. In order to relate the quenched fraction p to the experimentally known quantity ρ_S one evaluates the former as $p=l_b a_S \rho_S$, where a_S is the specific surface area of the aerosil and l_b is the boundary layer thickness [12].

From a study of the mixtures of 8CB and Degussa-type 300 aerosils [12] it follows that several predictions of these models are not consistent with experimental observations. The difficulties of the two former models can apparently be avoided in a third model, based on surface-induced order that converts the isotropic phase into a paranematic phase at the aerosil interface [12]. This model does not suppose a nonordering, quenched fraction of the liquid crystal. Instead one considers the boundary layer order to be Q_b so the volume-averaged order at T_{NI} for the coexisting nematic and isotropic phase is obtained as

$$\overline{Q_N}(p)=Q_N(0)(1-p)+Q_b p, \tag{5}$$

$$\overline{Q_I}(p)=Q_I(0)(1-p)+Q_b p, \tag{6}$$

where $Q_I(0)=0$ and $Q_N(0)$ are, respectively, the isotropic and the nematic bulk order parameters at T_{NI}. Using the mean-field expression for the latent heat one obtains

$$\begin{aligned}\Delta H_L(p)&=\frac{a_0}{2}[\overline{Q_N}^2(p)-\overline{Q_I}^2(p)]T_{NI}(p)\\&=\Delta H_L(0)(1-p)^2\left[1+\frac{2Q_b p}{Q_N(0)(1-p)}\right]\\&\quad\times\left(1-\frac{\Delta T_{NI}(p)}{T_{NI}(0)}\right),\end{aligned} \tag{7}$$

where $\Delta T_{NI}(p)=T_{NI}(0)-T_{NI}(p)$. This gives a decrease as a function of p, where the latent heat vanishes as soon as $Q_b/Q_N=(p-1)/2p\leqslant 0$ or else in the case $p=1$ (i.e., where $\overline{Q_I}=\overline{Q_N}=Q_b$).

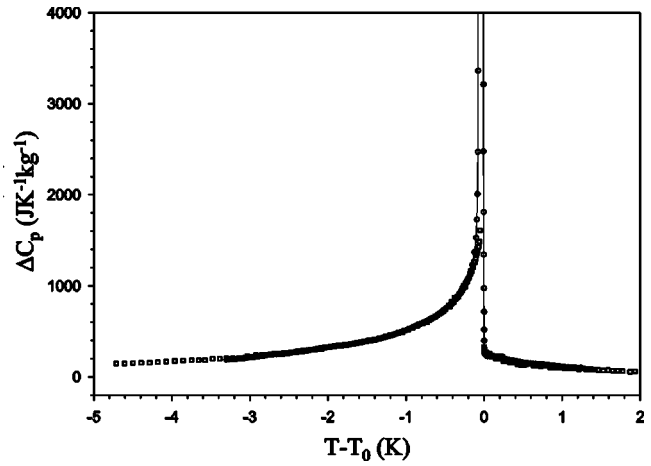

FIG. 1. Specific heat capacity of pure 7CB (interconnected dots), compared with the pretransition data of the reference measurement of Ref. [31] (open squares). Specific heat capacity and temperature values have been shifted over an appropriate value to allow for comparison with 7CB+aerosil mixtures. One can observe a very good agreement between both, except for a somewhat larger broadening in the present data at the transition (see text).

V. CALORIMETRIC RESULTS

When looking at the specific heat capacities of the samples, the appropriate quantity to consider is the sample heat capacity per mass of liquid crystal (not per sample mass). The reason for this is twofold: first, all phase transition behavior, in which we are interested, is due to the liquid crystal, while second, the aerosils only give an additional contribution to the background value of the sample heat capacity, this contribution obviously being proportional to the mass of aerosils present in the sample.

As a reference for this specific heat, we use a high-quality measurement of pure 7CB, where a large quantity (6.5766 g) of a high purity research sample, obtained from British Drug House (BDH), was investigated, entailing a value $T_{NI}=42.73\,^{\circ}\mathrm{C}$ for the NI transition temperature and a latent heat of $\Delta H_L=2087\pm 14$ J/kg [31]. This measurement gives a very good agreement with the pretransition of our measurement on pure 7CB (see Fig. 1), when a downward temperature shift of 0.14 K has been applied on the latter. This offset is most likely due to a thermometer scale difference between the different experimental setups used.

In a similar system (8CB+Degussa-type 300 aerosils), the aerosil content did not influence the pretransitional specific heat capacity of the NI transition [12]. Supporting these results, the pretransition for the pure, 0.096, and 0.15 samples overlaps well (see Fig. 2). However, a substantial broadening of the transition at the low temperature side of about 1 K is observed, which seems to be slightly more pronounced for the 0.15 mixture. For the 0.27 and 0.42 samples, this even extends over about 2 K, while the pretransitional excess specific heat capacity in the isotropic phase corresponds to that

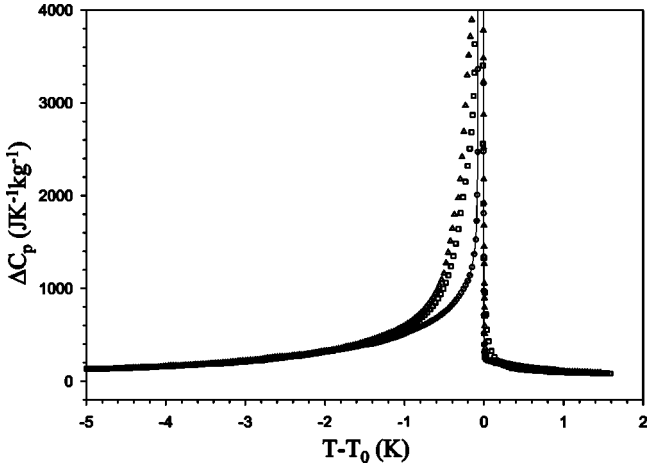

FIG. 2. Excess specific heat capacity for 7CB+aerosil mixtures: $\rho_S=0.096$ (squares), $\rho_S=0.15$ (triangles) compared with pure 7CB (interconnected dots).

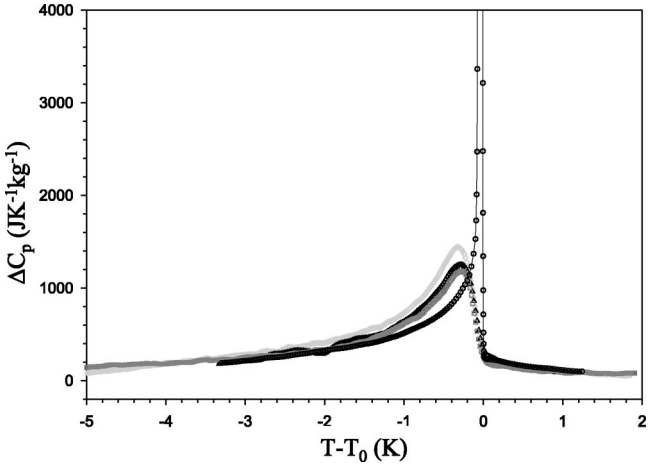

FIG. 4. Excess specific heat capacity for 7CB+aerosil mixtures: $\rho_S=0.57$ (gray squares), $\rho_S=0.58$ (black triangles), $\rho_S=0.66$ (light gray diamonds) compared with pure 7CB (interconnected dots).

of pure 7CB (see Fig. 3), as it does with the 0.57, 0.58, and 0.66 mixtures (see Fig. 4). Still, some broadening does seem to be characteristic for liquid crystal-aerosil mixtures (typically 0.2 K for the 8CB mixtures in Ref. [12]) but certainly not to the extent of our observations.

These observations are not consistent with the PBL and the RF model, both predicting a decrease of the pretransitional specific heat capacity with increasing quenched fraction p thus with increasing aerosil density. Based upon these experimental results, it seems that any model that assumes a fully quenched fraction p, such as the PBL and the RF model, is not valid. In order to evaluate this fraction p we must know the specific area of the aerosils for which a value of $a_S=300\ \mathrm{m^2\,g^{-1}}$ for Degussa-type 300 Aerosil is provided by the manufacturer [28]. Recent experimental results, however, show that at higher aerosil densities one must take into account that some surface area is lost due to multiple connections, hence decreasing the aerosil specific surface area. From an x-ray study it was found that the specific area is well described by the expression $a_S=300-103.8\rho_S\ \mathrm{m^2\,g^{-1}}$ [32]. Together with an estimate of $l_b\approx 20$ Å for 7CB [37] one finds that $p=l_b a_S\rho_S\approx 0.6\rho_S(1+0.346\rho_S)$.

Furthermore, a small additional peak superposed on the low temperature side of the main heat capacity peak was observed in the $\rho_S=0.096$ and 0.151 samples, however only on cooling. These additional features are reproducible (see Fig. 5). At higher ρ_S, however, (i.e., $\rho_S=0.267$ and above), no additional features were present on heating nor on cooling. Possibly this is similar to a doubling of the C_p peak in the $N+I$ coexistence observed for lower aerosil concentrations, and which becomes less pronounced with increasing ρ_S [12]. It has been suggested that this might be attributed to elastic coarsening where a conversion to nematic phase of some residual nonnematic liquid crystal very near the silica strands occurs below the actual NI transition [12]. The reasons as to why these features are much smaller in our measurements, and why they only occur upon cooling, are not clear.

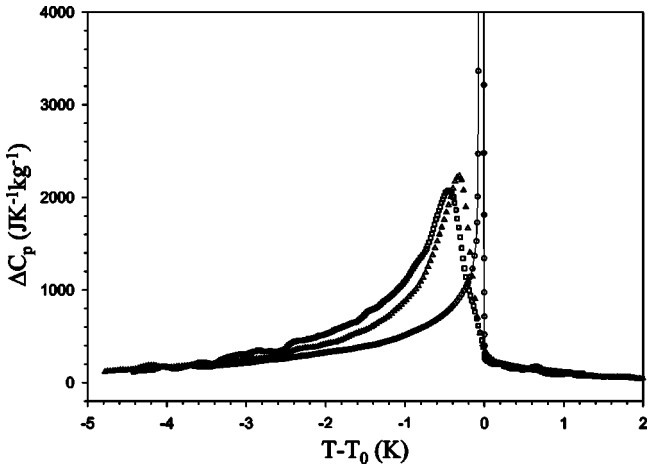

FIG. 3. Excess specific heat capacity for 7CB+aerosil mixtures: $\rho_S=0.27$ (squares), $\rho_S=0.42$ (triangles) compared with pure 7CB (interconnected dots).

VI. TRANSITION TEMPERATURES

For the mean-field surface-induced order model the transition temperature shift $\Delta T_{NI}(p)$ still has to be evaluated. It has been suggested that at very low ρ_S the RF model is a viable approximation: the aerosil strains can move around in the sample and anneal elastic strains, thus achieving relatively large nematic domains randomly oriented by an aerosil strand within them, while at higher ρ_S this shift can be modeled through an elastic-strain (ES) approach. However, for 7CB and 8CB it has been found that even for very low aerosil fractions ($\rho_S=0.005$) the transition temperature shift is already slower than that predicted by the RF model [12,13]. It must further be noted that the PBL model does not predict a transition temperature shift, in contradiction to experiment. The ES approach yields a transition temperature shift of

$$\Delta T_{NI}(p)=\frac{K}{2a_0}\left(\frac{2\pi}{R}\right)^2, \tag{8}$$

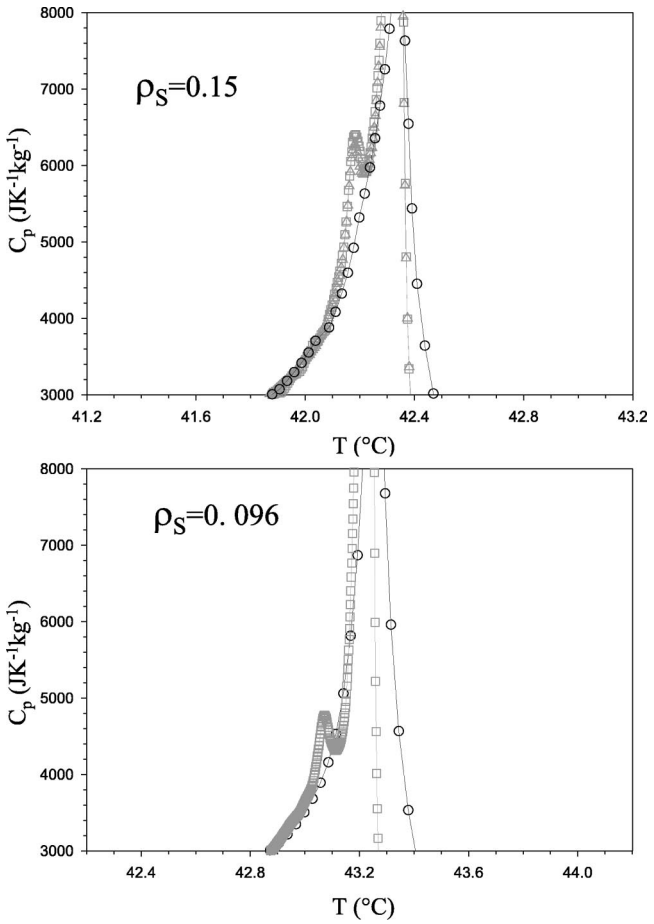

FIG. 5. Detail of the specific heat capacity (per mass of liquid crystal) of $\rho_S=0.15$ and $\rho_S=0.096$. A reproducible feature is observed only on cooling, not on heating. $\rho_S=0.15$, heating (black circles) and two cooling runs (gray squares and triangles); $\rho_S=0.096$, heating (black circles) and cooling (gray squares).

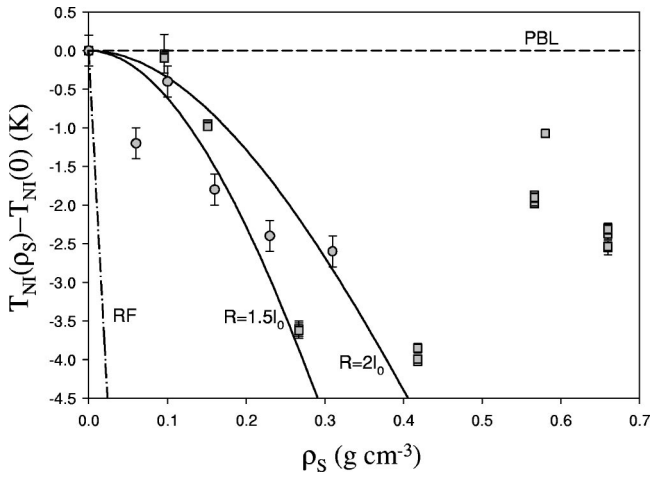

FIG. 6. The evolution of the transition temperature shift $T_{NI}(\rho_S)-T_{NI}(0)$ as a function of the aerosil density ρ_S: ASC data (squares) and the data of the dielectrical study of Ref. [17] (circles). The pinned boundary layer (PBL) model (dashed line) predicts no change in T_{NI} contrary to observation, while the random field (RF) model (dash-dot line) yields too rapid a variation. An elastic strain (ES) approach (full lines) where the radius of curvature of the aerosil voids is chosen $R=1.5l_0$ or $R=2l_0$ models this evolution fairly well up to about $\rho_S=0.4$. For aerosil concentrations above $\rho_S=0.5$, which, as explained in the text, are expected not to be fully homogeneous, R values of $4l_0$ to $5l_0$ would be needed to make the (reduced) temperature decrease compatible with the ES model.

K being the Frank elastic constant and R the radius of curvature of the elastic distortions [33].

As the most reliable measure of the NI transition temperature, we plotted the high temperature boundary of the NI coexistence region which, in contrast to its lower temperature counterpart, could be clearly obtained from enthalpy change plots. When compared to the results of Ref. [17] on the same kind of mixtures (see Fig. 6), we obtain reasonable agreement for values up to $\rho_S\approx 0.4$, when taking into account an accuracy of about 0.1 K on transition temperatures. However, some peculiar behavior of the measured T_{NI} occurs, mainly at higher ρ_S.

As was already pointed out in Ref. [12], taking R equal to the mean aerosil void size $l_0=2/a_S\rho_S$ yields too fast a decrease of T_{NI}. Supposing $R>l_0$, which yields a slower variation, is reasonable in view of the tendency of the liquid crystal material to minimize elastic strain hence promoting a larger radius of curvature. When taking 7CB values of $K\approx 5.0\times 10^{-11}N$ [34] and $a_0\approx 15\ 10^4\,\mathrm{J\,K^{-1}\,m^{-3}}$ [38], so $\Delta T_{NI}=6.58\times 10^{-15}/R^2$, reasonable agreement is obtained between experimental transition temperature shifts of both the results of Ref. [17] and of our ASC experiments for $\rho_S<0.4$, and the theoretical prediction of Eq. (8) taking $R=1.5l_0$ or $R=2l_0$, without the need for an empirical temperature offset as in Ref. [12]. However, transitions for $\rho_S>0.4$ lie at substantially higher temperatures than those predictions. At $\rho_S>0.5$ even a value of about $R=4l_0$ results from those data points. Finally, one notices that the transition temperatures of the $\rho_S=0.57$ and $\rho_S=0.58$ mixture differ by about 0.8 K. Since ASC experiments were reproducible for each mixture, the cause for this behavior most likely relates to the (preparation of the) samples themselves.

A possible explanation could be that the transition temperatures are affected by the presence of some impurities, originating from the acetone used in sample preparation (which contains typically 0.2% of water). However, one would expect that this would generally decrease T_{NI} [35]. This phenomenon does not occur at the $\rho_S>0.5$ samples, which have a noticeably higher T_{NI} than would be expected according to Eq. (8) even when taking $R=2l_0$.

A more viable explanation would follow from the consideration that one should distinguish between two different effects: first, the decrease of the transition temperature which is affected by a diminishing radius of curvature R of the elastic distortions, being closely related to the mean void size l_0, and second, the decrease of latent heat, which is affected by an increasing surface of the aerosil strands. It is observed that transition temperatures at higher ρ_S generally lie higher than expected from ES predictions, while integrated specific heat capacity values and the latent heats derived thereof seem to decrease as expected (see Fig. 8 and further discussion in Sec. VII). The former implies a larger radius of cur-

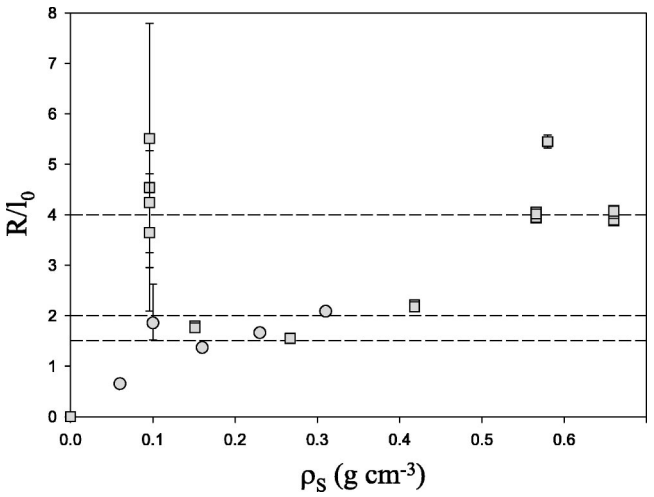

FIG. 7. Evolution of the radius of curvature R of the aerosil voids compared to the average void size l_0 as a function of ρ_S: ASC data (squares) and the data of the dielectrical study of Ref. [17] (circles). Further details: see text.

vature than expected at this ρ_S, and an accordingly larger mean void size. The latter implies that the total surface of the aerosil strands is as expected. Both these observations do not necessarily contradict each other: one could imagine a unit volume containing a smaller number of larger voids present instead of a larger number of smaller voids, the latter having smaller radius of curvature but still a comparable total surface. As a consequence, the latent heat would essentially remain unaffected. We note that in Ref. [12] a constant ratio of $R/l_0=5$ gave good agreement with transition temperature shifts. This value of R/l_0 had no effect on the behavior of the integrated transition heat $\delta H+\Delta H$.

Information on the behavior of the ratio R/l_0 can be obtained by comparing the experimental value ΔT_{NI}^{exp}, which is considered to be described by Eq. (8), and the predicted value assuming $R=l_0$, which is $\Delta T_{NI}^{R=l_0}=K/2a_0(2\pi/l_0)^2$. This yields

$$\frac{R}{l_0}=\sqrt{\frac{\Delta T_{NI}^{R=l_0}}{\Delta T_{NI}^{exp}}}, \tag{9}$$

the results of which are plotted as a function ρ_S in Fig. 7.

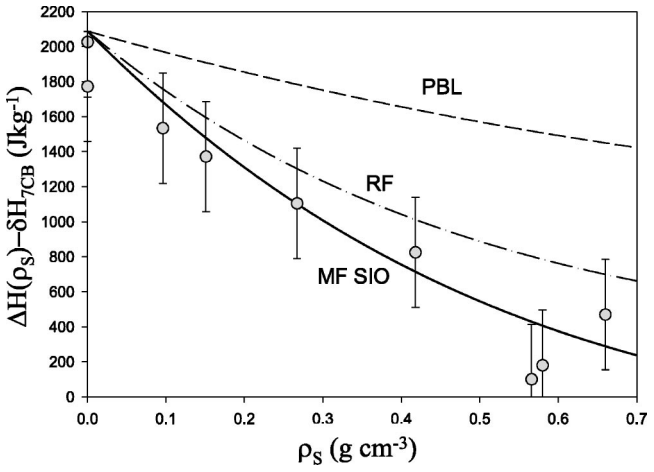

FIG. 8. Evolution of the latent heat as a function of aerosil density: pinned boundary layer (PBL) model (dashed line), random field (RF) model (dash-dot line) and a mean-field surface-induced order (MF SIO) model with one adjustable parameter $Q_b/Q_N=-0.8\pm0.3$ obtained through fitting (full line). Comparison is made to experimentally obtained values (circles). Further details can be found in Sec. VII.

A possible mechanism for obtaining such a void distribution could be that at high ρ_S the amount of acetone used for dissolving both aerosils and liquid crystal, was not large enough and/or the sonification time was not sufficiently long. One must note that the individual aerosil particles form aggregates, which then bind together to form agglomerates that lead to the aerosil network of complex geometries [36]. As a consequence, when not all of the aerosils are completely and homogeneously dissolved, one could conceive that this would lead to larger agglomerates forming larger, but fewer aerosil strands. Accordingly the formation of larger voids filled with liquid crystal would be favored in comparison with the case where all of the aerosils would be properly dissolved (i.e. where the agglomerates would generally be smaller). The tendency of the liquid crystal to minimize elastic strain, i.e., to maximize the radius of curvature, would also favor this kind of configuration. This behavior would be more likely to occur at large aerosil concentrations.

The rather large values of R/l_0 between 4 and 5 needed for our $\rho_S>0.5$ results, when compared to values roughly between 1.5 and 2 for $0.2<\rho_S<0.5$ (see Fig. 7) again correspond to what has been argued. It is commonly observed that transition temperatures in the low-ρ_S region (i.e., $\rho_S<0.1$) are not well described by an ES approach, which explains the rather small R/l_0 value in Fig. 7 for $\rho_S=0.06$ of Ref. [17]. The fairly large value of our 0.096 mixture, is probably related to sample preparation, since a mixture of approximately the same aerosil content of Ref. [17] behaves as expected, keeping in mind that estimates of R/l_0 at such a small ΔT_{NI} value are rather uncertain.

When comparing the 0.57 and 0.58 mixture, we notice that the latter has a considerably higher transition temperature while at the same time both have approximately the same latent heat value. However, the amount of acetone used for the 0.58 mixture was less than that used for the 0.57 mixture, which fits our explanation. Moreover, this shows that these latent heat values are reliable. The unusually large broadening observed at lower ρ_S might accordingly be explained by the presence of a relatively small (when compared to high ρ_S mixtures) amount of aerosil which is not properly (homogeneously) dissolved, thus creating some local variations in density across the sample, resulting in a distribution of transition temperatures, but not to the extent that a noticeable influence on the (average) transition temperature is observed. Finally, one must notice that this problem would naturally be more prevalent where larger quantities of sample are prepared and/or examined (i.e., in our ASC measurements).

VII. TRANSITION HEATS

Normally the latent heat would be determined as the magnitude of the discontinuous jump in the plot of the enthalpy as a function of temperature. Unfortunately, this procedure cannot be used in this case: the latent heat onset on the low temperature side cannot clearly be located due to the already mentioned broadening. As a consequence, a more indirect technique has to be used to extract latent heat values. The surface below the $C_s(T)/m_{LC}$ curve, obtained by a numerical integration over an appropriately chosen temperature interval, is compared with the surface of the pretransitional specific heat curve of pure 7CB over the same interval. If the pretransition remains constant, the difference between both yields the latent heat for a given mixture. If this assumption is not valid, the change of the pretransition is also included in this value, i.e., one obtains $\Delta H(\rho_S)-\delta H_{7CB}=\Delta H_L(\rho_S)+[\delta H(\rho_S)-\delta H_{7CB}]$, where $\Delta H(\rho_s)$, $\delta H(\rho_s)$ refer to the total transition heat and the pretransition of a mixture with aerosil density ρ_S.

As a test of its accuracy, this method was applied to the data of the pure 7CB sample we investigated. We derived a value of $\Delta H_L=2030\ \mathrm{J\,kg^{-1}}$ upon cooling and $\Delta H_L=1770\ \mathrm{J\,kg^{-1}}$ upon heating. The latter differs by about $315\ \mathrm{J\,kg^{-1}}$ with the reference value of $\Delta H_L=2087\pm 14\ \mathrm{J\,kg^{-1}}$ from Ref. [31] (a relative error of about 15%). For our pure 7CB data, a direct determination of the latent heat from the $H(T)$ curve was possible which yields a much more accurate value $\Delta H_L=2060\pm 50\ \mathrm{J\,kg^{-1}K^{-1}}$. This difference of $315\ \mathrm{J\,kg^{-1}}$ seems an appropriate value for the error on the obtained latent heat values when deduced in the above described indirect way. Indeed, one must keep in mind that the derived latent heat is a quite small difference between two relatively large values for the total surface of the $C_s(T)/m_{LC}$ curve. Additionally, the C_s values are somewhat dependent on the details of the numerical determination of dT/dt. This is especially noticeable very near to the transition temperature for low ρ_S, where these values are very high, thus any relatively small rounding error would cause a relatively large effect in the absolute value. Evidently, since transition peaks at higher ρ_S are more rounded, they would suffer less from this effect.

Qualitatively, the values obtained through this method show a gradual decrease with ρ_S similar to that of previously investigated liquid crystal-aerosil system [12], which does not seem to be affected much by the previously described peculiar behavior of the transition temperatures (see Fig. 8), supporting our explanation in Sec. VI.

It must be noted that, even though the RF model shows a fair correspondence of its predicted latent heat with experiment, it entails an additional decrease of the pretransition, not supported by experiment, which is not included in the theoretical curve $\Delta H_L(p)=(1-p)^3\Delta H_L(0)$ shown in Fig. 8. The same is true for the PBL model, which additionally yields a latent heat curve that does not show a sufficiently pronounced decrease.

When we insert predicted values for $\Delta T_{NI}(p)$ using $R=2l_0$ into Eq. (7), we obtain an expression for $\Delta H_L(p)$ with only one adjustable parameter $Q_b/Q_N(0)$. Fitting experimental values to this expression yields a value of $Q_b/Q_N(0)=-0.8\pm 0.3$. The negative sign of this parameter corresponds to an ''escaped radial'' configuration of the director: it is homeotropically aligned near the aerosil surface (Q_b is negative), whilst being parallel to the aerosil strands inside the voids [$Q_N(0)$ is positive] [12]. Upon insertion of a typical value of $Q_N(0)\approx 0.3$ this yields $Q_b\approx -0.3\pm 0.1$, which is of the same sign and order of magnitude as the value $Q_b=-0.15$ of Ref. [12]. Thus the latent heat would vanish at $p\approx 0.38$, i.e., near $\rho_S\approx 1$ according to this model. As can be seen on Fig. 8, experimental results are well described by this model.

VIII. CONCLUSION

Adiabatic scanning calorimetry was employed to make a systematic study of the nematic to isotropic transition in mixtures of the liquid crystal 7CB with hydrophilic aerosil particles. Mixtures have been investigated with an aerosil content between $\rho_S=0.1$ and $\rho_S=0.7$, the latter being substantially higher than that investigated in previous studies with other liquid crystal-aerosil mixtures. We obtained information about transition temperatures and transition heats of the investigated transition.

While the transition heats decreased with increasing ρ_S as was expected, some peculiar behavior of the transition temperatures was observed, together with an unusually large broadening of the transitions. It has been suggested that this can be explained, in the context of the elastic strain (ES) approach usually employed to describe transition temperature shifts, by variations in the distribution of the radius of curvature R of the aerosil voids originating from sample preparation. It is important in this regard to separate two effects, i.e., the behavior of the transition temperatures and the transition (latent) heats, the former being influenced by the radius of curvature R of the voids and the latter by the total void surface per unit volume.

Latent heat values could not be determined directly from the enthalpy versus temperature curve because of the large broadening of the transition. Instead, an indirect method had to be used consisting in the comparison of the integrated heat capacity per mass of liquid crystal with the pretransition of a reference measurement of pure 7CB [31]. The evolution of these values as a function of ρ_S, which remains essentially unaffected by the aforementioned temperature variations, was compared to the predictions of several theoretical models.

The pinned boundary layer (PBL) model does not predict a transition temperature shift, in contradiction to experiment. Furthermore, it yields too slow a variation of the latent heat. The random field (RF) model predicts a far too rapid transition temperature decrease. Even though latent heat values predicted by this model give fair agreement to our experimentally obtained values, it—as well as the PBL model—supposes a strongly anchored surface layer at the aerosil strands thus a fraction p of the liquid crystal [with $p\approx 0.6\rho_s(1+0.346\rho_S)$ for 7CB] which is not participating in any transition. As a consequence, a decrease of the pretran-

sition with a factor $1-p$ is predicted. This, however, is not supported by experiment.

Good agreement was obtained with a mean-field surface-induced order approach as proposed in Ref. [12], where a paranematic surface layer with order parameter Q_b is supposed at the aerosil strands in both the nematic and the isotropic phase. This avoids the difficulties arising from the previously mentioned theories and gives an expression for the latent heat decrease with only one adjustable parameter, for which a fitted value of $Q_b/Q_N=-0.8\pm0.3$ is obtained. This yields a value of $Q_b=-0.3\pm0.1$ and accordingly the latent heat is predicted to vanish near $\rho_S\approx1$.

ACKNOWLEDGMENT

This work was supported by the Fund for Scientific Research Flanders (Belgium) (FWO, Project No. G.0264.97N).

[1] P.G.D. Gennes and J. Prost, *The Physics of Liquid Crystals*, 2nd ed. (Clarendon, Oxford, 1993).
[2] G. Vertogen and W.D. Jeu, *Thermotropic Liquid Crystals* (Springer-Verlag, Berlin, 1988).
[3] J. Thoen, Int. J. Mod. Phys. B **9**, 2157 (1995).
[4] *Liquid Crystals in Complex Geometries Formed by Polymer and Porous Networks*, edited by G.P. Crawford and S. Zumer (Taylor & Francis, London, 1996).
[5] L. Wu, B. Zhou, C.W. Garland, T. Bellini, and C.W. Schaeffer, Phys. Rev. E **51**, 2157 (1995).
[6] Z. Kutnjak and C.W. Garland, Phys. Rev. E **55**, 488 (1997).
[7] B. Zhou, G.S. Iannacchione, and C.W. Garland, Liq. Cryst. **22**, 335 (1997).
[8] H. Haga and C.W. Garland, Liq. Cryst. **22**, 275 (1997).
[9] H. Haga and C.W. Garland, Liq. Cryst. **23**, 645 (1997).
[10] H. Haga and C.W. Garland, Phys. Rev. E **56**, 3044 (1997).
[11] B. Zhou, G.S. Iannacchione, C.W. Garland, and T. Bellini, Phys. Rev. E **55**, 2962 (1997).
[12] G.S. Iannacchione, C.W. Garland, J.T. Mang, and T.P. Rieker, Phys. Rev. E **58**, 5966 (1998).
[13] F. Mercuri, A.K. Ghosh, and M. Marinelli, Phys. Rev. E **60**, R6309 (1999).
[14] M. Marinelli, A.K. Ghosh, and F. Mercuri, Phys. Rev. E **63**, 061713 (2001).
[15] T. Bellini, N.A. Clark, V. Degiorgio, F. Mantegazza, and G. Natale, Phys. Rev. E **57**, 2996 (1998).
[16] T. Bellini, M. Buscaglia, C. Chiccoli, F. Mantegazza, P. Pasini, and C. Zannoni, Phys. Rev. Lett. **85**, 1008 (2000).
[17] A. Hourri, T.K. Bose, and J. Thoen, Phys. Rev. E **63**, 051702 (2001).
[18] S. Tschierke, O.V. Yaroshuk, and H. Kresse, Cryst. Res. Technol. **30**, 571 (1995).
[19] S.L. Abd-El-Messieh, J. Werner, H. Schmalfuss, W. Weisflog, and H. Kresse, Liq. Cryst. **26**, 535 (1999).
[20] S. Frunza, A. Frunza, H. Goering, H. Sturm, and A. Schönhals, Europhys. Lett. **56**, 801 (2001).
[21] A. Hourri, P. Jamée, T.K. Bose, and J. Thoen, Liq. Cryst. **29**, 459 (2002).
[22] J. Thoen, H. Marynissen, and W.V. Dael, Phys. Rev. A **26**, 2886 (1982).
[23] P. Jamée, G. Pitsi, M.-H. Li, H.-T. Nguyen, G. Sigaud, and J. Thoen, Phys. Rev. E **62**, 3687 (2000).
[24] M. Young, G. Pitsi, M.-H. Li, H.-T. Nguyen, P. Jamée, G. Sigaud, and J. Thoen, Liq. Cryst. **25**, 387 (1998).
[25] A. Cruz-Orea, G. Pitsi, P. Jamée, and J. Thoen, J. Agric. Food Chem. **50**, 1335 (2002).
[26] G. Pitsi, J. Caerels, and J. Thoen, Phys. Rev. B **55**, 915 (1997).
[27] J. Thoen, in *Physical Properties of Liquid Crystals*, edited by D. Demus, J. Goodby, G. Gray, H.-W. Spiess, and V. Vill (Wiley-VCH, Weinheim, 1997), pp. 208–232.
[28] Degussa Corp., Silica Division, 65 Challenger Road, Ridgefield Park, NJ 07660 USA. Technical data and properties are given in the manufacturers manual AEROSILS.
[29] A. Maritan, M. Cieplak, T. Bellini, and J.R. Banavar, in *Liquid Crystals in Complex Geometries Formed by Polymer and Porous Networks* (Ref. [4]), Chap. 22, pp. 483–496.
[30] A. Maritan, M. Cieplak, and J.R. Banavar, Phys. Rev. Lett. **72**, 4113 (1994).
[31] F. Detremmerie, Licentiaatsthesis, Katholieke Universiteit Leuven, 1983.
[32] G.S. Iannacchione (private communication).
[33] D. Finotello, G.S. Iannacchione, and S. Qian, in *Liquid Crystals in Complex Geometries Formed by Polymer and Porous Networks* (Ref. [4]), Chap. 16, pp. 325–343.
[34] R. Stannarius, in *Handbook of Liquid Crystals*, edited by D. Demus, J. Goodby, G.W. Gray, H.-W. Spiess, and V. Vill (Wiley-VCH, Weinheim, 1998), Vol. 2A, Chap. 2.1.
[35] M.A. Anisimov, *Critical Phenomena in Liquids and Liquid Crystals* (Gordon and Breach, Philadelphia, 1991).
[36] M. Kreuzer, and R. Eidenschink, in *Liquid Crystals in Complex Geometries Formed by Polymer and Porous Networks* (Ref. [4]), Chap. 15, pp. 307–324.
[37] An estimated value of $l_b\approx20$ Å was used for 8CB in Ref. [12]. This seems to hold as an appropriate estimate for 7CB, since the latter has nearly the same chemical composition as 8CB.
[38] Literature values are available for 5CB, $a_0=9\times10^4$ J K^{-1} m^{-3} [33], and for 8CB, $a_0=18\times10^4$ J K^{-1} m^{-3} [12]. For 7CB one must resort to an estimate using the mean-field formula $\Delta H_L/T_{NI}=2a_0B^2/9C^2$ [35]. Assuming that B and C will not change significantly for members of the same homologous series, one can then estimate $a_0^{7CB}\approx(\Delta H_L^{7CB}/T_{NI}^{7CB})(T_{NI}/\Delta H_L)a_0$, where a_0, ΔH_L, and T_{NI} are values from another member of the homologous series. Using 5CB values of $T_{NI}=308$ K and $\Delta H_L=389.5$ J mol^{-1} [31] yields $a_0^{7CB}\approx13\times10^4$ J K^{-1} m^{-3} and using 8CB values $T_{NI}=314$ K and $\Delta H_L\approx600$ J mol^{-1} one obtains $a_0^{7CB}\approx17\times10^4$ J K^{-1} m^{-3}. Thus a 7CB value of $a_0\approx15\times10^4$ J K^{-1} m^{-3} seems appropriate.